Northumbria Research Link

Northumbria
University
NEWCASTLE

University**Library**

Free vibration of axially loaded composite beams using a four-unknown shear and normal deformation theory

Thuc P. Vo[a,b], Huu-Tai Thai[c,d,e,*], Metin Aydogdu[f]

[a]*Faculty of Engineering and Environment, Northumbria University, Newcastle upon Tyne, NE1 8ST, UK*
[b]*Institute of Research and Development, Duy Tan University, 03 Quang Trung, Da Nang, Vietnam*
[c]*Division of Construction Computation, Institute for Computational Science, Ton Duc Thang University, Ho Chi Minh City, Vietnam*
[d]*Faculty of Civil Engineering, Ton Duc Thang University, Ho Chi Minh City, Vietnam*
[e]*School of Engineering and Mathematical Sciences, La Trobe University, Bundoora, VIC 3086, Australia*
[f]*Department of Mechanical Engineering, Trakya University, 22030 Edirne, Turkey*

Abstract

This paper presents free vibration of composite beams under axial load using a four-unknown shear and normal deformation theory. The constitutive equation is reduced from the 3D stress-strain relations of orthotropic lamina. The governing differential equations of motion are derived using the Hamilton's principle. A two-node C^1 beam element is developed by using a mixed interpolation with linear and Hermite-cubic polynomials for unknown variables. Numerical results are computed and compared with those available in the literature and commercial finite element software (ANSYS and ABAQUS). The comparison study illustrates the effects of normal strain, lay-ups and Poisson's ratio on the natural frequencies and load-frequency curves of composite beams.

Keywords: Composite beams; normal strain; Poisson effect; shear and normal deformation theory

1. Introduction

Due to the attractive properties of strength, stiffness, and lightness, composite structures become popular in several applications of aerospace, automotive, civil engineering, etc. In particular, composite beams are widely used and thus many beam theories have been proposed to predict their free vibration and dynamic response. Finite element models originally developed for solid mechanics and mainly for isotropic beams have been extended to laminated composite ones by many authors and only some of them are referenced here ([1–6]). More details can be found in recent review by Sayyad and Ghugal [7]. These models provide reasonably accurate results for the structural response of thin to moderately thick composite beams. Because of the low shear moduli of composite materials, the effect of shear deformation is expected to be much more pronounced in composite beams than in the

---

*Corresponding author.
E-mail addresses: thuc.vo@northumbria.ac.uk (T.P. Vo), thaihuutai@tdt.edu.vn (H.-T. Thai)

homogeneous ones. In order to obtain more accurate results for the free vibration analysis of composite beams, many investigators have used either the first-order [8, 9] or higher-order beam theories ([10–19]). However, these mentioned studies do not take into account the effect of normal strain which can be significant for thick composite beams. This effect can be included when both variations of in-plane and out-of-plane displacements are assumed to be higher-order through the beam depth. These beam models are normally called quasi-3D theory. Carrera et al. ([20–22]) proposed a novel unified approach called Carrera Unified Formulation, in which the effects of shear and normal deformation were automatically included to investigate free vibration of composite beams. These effects were also taken into account by Matsunaga [23] to analyse vibration and buckling responses of cross-ply simply-supported beams using Navier solution. Vidal and Polit [24] used sinus finite elements with normal stress for vibration of multilayered beams. Recently, Mantari and Canales [25, 26] derived the Ritz solution for vibration and buckling analysis of composite beams based on a generalized quasi-3D theory. It should be noted that above studies [23–26] do not consider the Poisson effect, which needs to be included to predict accurately behaviour of composite beams with general lay-ups [27, 28]. Marur and Kant [29] formulated a higher order beam theory, which included shear and normal strain and derived isoparametric 1D finite element for vibration of angle-ply beams. Li et al. [30] investigated the influences of shear, normal strain and Poisson effect on vibration of simply-supported composite beams using Navier solution. Apparently, this complicated problem for composite beams with arbitrary lay-ups for various boundary conditions is under-researched.

This paper, which is extended from previous research [31, 32], presents a free vibration of composite beams under axial load. It is based on a quasi-3D theory, in which in-plane and out-of-plane displacements are assumed to be third-order and second-order polynomial through the beam depth. Thus, it has parabolic distribution of the shear strain and includes the normal strain effect. The constitutive equation is reduced from the 3D stress-strain relationship of an orthotropic lamina. The governing differential equations of motion are derived using the Hamilton's principle. A two-node C^1 beam element is develop to solve the problems. Several numerical examples are carried out and compared with those available in the literature and commercial finite element software (ANSYS and ABAQUS). The effects of normal strain, lay-ups, Poisson's ratio and span-to-height ratios on the natural frequencies and load-frequency curves of composite beams are investigated.

2. Theoretical Formulation

2.1. Kinetic and constitutive equations

A composite beam with rectangular cross-section $b \times h$ and length L is shown in Fig. 1. It is composed of orthotropic multilayers with fibre angle with respect to the x-axis. The in-plane and out-plane displacements are assumed to be third-order and second-order polynomial through the beam depth [31–33]:

$$U(x,z,t) = u(x,t) - z\frac{\partial w_b(x,t)}{\partial x} - \frac{4z^3}{3h^2}\frac{\partial w_s(x,t)}{\partial x} = u(x,t) - zw_b'(x,t) - f(z)w_s'(x,t) \quad (1a)$$

$$W(x,z,t) = w_b(x,t) + w_s(x,t) + (1 - \frac{4z^2}{h^2})\phi_z(x,t) = w_b(x,t) + w_s(x,t) + g(z)\phi_z(x,t) \quad (1b)$$

where u, w_b, w_s and ϕ_z are four unknown displacements of the mid-plane of the beam.

The axial, normal and shear strains are given by:

$$\epsilon_x = \frac{\partial U}{\partial x} = u' - zw_b'' - fw_s'' \quad (2a)$$

$$\epsilon_z = \frac{\partial W}{\partial z} = g'\phi_z \quad (2b)$$

$$\gamma_{xz} = \frac{\partial W}{\partial x} + \frac{\partial U}{\partial z} = g(w_s' + \phi_z') \quad (2c)$$

The stress-strain relationship of a kth orthotropic lamina are given by:

$$\left\{ \begin{array}{c} \sigma_x \\ \sigma_z \\ \sigma_{xz} \end{array} \right\}^k = \left[\begin{array}{ccc} \overline{Q}_{11}^* & \overline{Q}_{13}^* & 0 \\ \overline{Q}_{13}^* & \overline{Q}_{33}^* & 0 \\ 0 & 0 & \overline{Q}_{55}^* \end{array} \right]^k \left\{ \begin{array}{c} \epsilon_x \\ \epsilon_z \\ \gamma_{xz} \end{array} \right\} \quad (3)$$

where

$$\overline{Q}_{11}^* = \overline{Q}_{11} + \frac{\overline{Q}_{16}^2\overline{Q}_{22} - 2\overline{Q}_{12}\overline{Q}_{16}\overline{Q}_{26} + \overline{Q}_{12}^2\overline{Q}_{66}}{\overline{Q}_{26}^2 - \overline{Q}_{22}\overline{Q}_{66}} \quad (4a)$$

$$\overline{Q}_{13}^* = \overline{Q}_{13} + \frac{\overline{Q}_{16}\overline{Q}_{22}\overline{Q}_{36} + \overline{Q}_{12}\overline{Q}_{23}\overline{Q}_{66} - \overline{Q}_{16}\overline{Q}_{23}\overline{Q}_{26} - \overline{Q}_{12}\overline{Q}_{26}\overline{Q}_{36}}{\overline{Q}_{26}^2 - \overline{Q}_{22}\overline{Q}_{66}} \quad (4b)$$

$$\overline{Q}_{33}^* = \overline{Q}_{33} + \frac{\overline{Q}_{36}^2\overline{Q}_{22} - 2\overline{Q}_{23}\overline{Q}_{26}\overline{Q}_{36} + \overline{Q}_{23}^2\overline{Q}_{66}}{\overline{Q}_{26}^2 - \overline{Q}_{22}\overline{Q}_{66}} \quad (4c)$$

$$\overline{Q}_{55}^* = \overline{Q}_{55} - \frac{\overline{Q}_{45}^2}{\overline{Q}_{44}} \quad (4d)$$

where $\overline{Q}_{ij}$ are the transformed reduced stiffness constants [34]. It should be noted that if the Poisson effect is neglected, $\overline{Q}_{ij}^*$ is replaced by $\overline{Q}_{ij}$ in stress-strain relationship.

2.2. Variational formulation

The variation of the strain energy $\delta\mathcal{U}$ of the system:

$$
\begin{aligned}
\delta\mathcal{U} &= \int_0^l \int_0^b \left[\int_{-h/2}^{h/2} (\sigma_x \delta\epsilon_x + \sigma_{xz}\delta\gamma_{xz} + \sigma_z g'\delta\phi_z)dz \right] dydx \\
&= \int_0^l \Big[(Au' - Bw_b'' - B_s w_s'' + X\phi_z)\delta u' - (Bu' - Dw_b'' - D_s w_s'' + Y\phi_z)\delta w_b'' \\
&\quad - (B_s u' - D_s w_b'' - H w_s'' + Y_s\phi_z)\delta w_s'' + A_s(w_s' + \phi_z')(\delta w_s' + \delta\phi_z') \\
&\quad + (Xu' - Y w_b'' - Y_s w_s'' + Z\phi_z)\delta\phi_z \Big])dx
\end{aligned}
\tag{5}
$$

where

$$
(A, B, B_s, D, D_s, H) = \int_{-h/2}^{h/2} \overline{Q}_{11}^*(1, z, f, z^2, fz, f^2, g'^2)bdz
\tag{6a}
$$

$$
(X, Y, Y_s) = \int_{-h/2}^{h/2} \overline{Q}_{13}^* g'(1, z, f)bdz
\tag{6b}
$$

$$
A_s = \int_{-h/2}^{h/2} \overline{Q}_{55}^* g^2 bdz
\tag{6c}
$$

$$
Z = \int_{-h/2}^{h/2} \overline{Q}_{33}^* g'^2 bdz
\tag{6d}
$$

The variation of the work done $\delta\mathcal{V}$ by the axial load P_0:

$$
\delta\mathcal{V} = -\int_0^l P_0 \Big[\delta w_b'(w_b' + w_s') + \delta w_s'(w_b' + w_s') \Big] dx
\tag{7}
$$

The variation of the kinetic energy $\delta\mathcal{K}$ of the system:

$$
\begin{aligned}
\delta\mathcal{K} &= \int_0^l \int_0^b \left[\int_{-h/2}^{h/2} \rho(\dot{U}\delta\dot{U} + \dot{W}\delta\dot{W})dz \right] dydx \\
&= \int_0^l \Big[\delta\dot{u}(m_0\dot{u} - m_1\dot{w}_b' - m_f\dot{w}_s') + \delta\dot{w}_b[m_0(\dot{w}_b + \dot{w}_s) + m_g\dot{\phi}_z] + \delta\dot{w}_b'(-m_1\dot{u} + m_2\dot{w}_b' + m_{fz}\dot{w}_s') \\
&\quad + \delta\dot{w}_s[m_0(\dot{w}_b + \dot{w}_s) + m_g\dot{\phi}_z] + \delta\dot{w}_s'(-m_f\dot{u} + m_{fz}\dot{w}_b' + m_{f^2}\dot{w}_s') \\
&\quad + \delta\dot{\phi}_z[m_g(\dot{w}_b + \dot{w}_s) + m_{g^2}\dot{\phi}_z] \Big] dx
\end{aligned}
\tag{8}
$$

where

$$
(m_0, m_1, m_2) = \int_{-h/2}^{h/2} \rho(1, z, z^2)bdz
\tag{9a}
$$

$$
(m_f, m_{fz}, m_{f^2}) = \int_{-h/2}^{h/2} \rho(f, fz, f^2)bdz
\tag{9b}
$$

$$
(m_g, m_{g^2}) = \int_{-h/2}^{h/2} \rho(g, g^2)bdz
\tag{9c}
$$

4

The weak form is derived by using Hamilton's principle:

$$0 = \int_{t_1}^{t_2} (\delta\mathcal{K} - \delta\mathcal{U} - \delta\mathcal{V})dt$$

$$
\begin{aligned}
0 = & \int_{t_1}^{t_2} \int_0^l \Big[\delta\dot{u}(m_0\dot{u} - m_1\dot{w_b}' - m_f\dot{w_s}') + \delta\dot{w_b}[m_0(\dot{w_b} + \dot{w_s}) + m_g\dot{\phi_z}] + \delta\dot{w_b}'(-m_1\dot{u} + m_2\dot{w_b}' + m_{fz}\dot{w_s}') \\
& + \delta\dot{w_s}[m_0(\dot{w_b} + \dot{w_s}) + m_g\dot{\phi_z}] + \delta\dot{w_s}'(-m_f\dot{u} + m_{fz}\dot{w_b}' + m_{f2}\dot{w_s}') + \delta\dot{\phi_z}[m_g(\dot{w_b} + \dot{w_s}) + m_{g2}\dot{\phi_z}] \\
& + P_0\big[\delta w_b'(w_b' + w_s') + \delta w_s'(w_b' + w_s')\big] - N_x\delta u' + M_x^b\delta w_b'' + M_x^s\delta w_s'' - Q_{xz}\delta w_s' - R_z\delta\phi_z \Big]dxdt
\end{aligned}
\tag{10}
$$

3. Solution procedure

A two-node C^1 beam element with six degree-of-freedom per node is developed. A mixed interpolation, which is linear polynomial Ψ_j for u and ϕ_z and Hermite-cubic polynomial ψ_j for w_b and w_s is used. The displacements within an element are expressed as:

$$u = \sum_{j=1}^{2} u_j\Psi_j \tag{11a}$$

$$w_b = \sum_{j=1}^{4} w_{bj}\psi_j \tag{11b}$$

$$w_s = \sum_{j=1}^{4} w_{sj}\psi_j \tag{11c}$$

$$\phi_z = \sum_{j=1}^{2} \phi_{zj}\Psi_j \tag{11d}$$

By substituting the above displacements into the weak form, Eq. (10), the finite element model can be obtained:

$$([K] - P_0[G] - \omega^2[M])\{\Delta\} = \{0\} \tag{12}$$

where

$$K_{ij}^{11} = \int_0^l A\Psi_i'\Psi_j'dx; \quad K_{ij}^{12} = -\int_0^l B\Psi_i'\psi_j''dx; \tag{13a}$$

$$K_{ij}^{13} = -\int_0^l B_s\Psi_i'\psi_j''dx; \quad K_{ij}^{14} = \int_0^l X\Psi_i'\Psi_j dx \tag{13b}$$

$$K_{ij}^{22} = \int_0^l D\psi_i''\psi_j''dx; \quad K_{ij}^{23} = \int_0^l D_s\psi_i''\psi_j''dx; \quad K_{ij}^{24} = -\int_0^l Y\psi_i''\Psi_j dx \tag{13c}$$

$$K_{ij}^{33} = \int_0^l (H\psi_i''\psi_j'' + A_s\psi_i'\psi_j')dx; \quad K_{ij}^{34} = \int_0^l (-Y_s\psi_i''\Psi_j + A_s\psi_i'\Psi_j')dx \tag{13d}$$

$$K_{ij}^{44} = \int_0^l (Z\Psi_i\Psi_j + A_s\Psi_i'\Psi_j')dx \tag{13e}$$

5

$$G_{ij}^{22} = \int_0^l \psi_i' \psi_j' dx; \quad G_{ij}^{23} = \int_0^l \psi_i' \psi_j' dx; \quad G_{ij}^{33} = \int_0^l \psi_i' \psi_j' dx \tag{13f}$$

$$M_{ij}^{11} = \int_0^l m_0 \Psi_i \Psi_j dx; \quad M_{ij}^{12} = -\int_0^l m_1 \Psi_i \psi_j' dx; \quad M_{ij}^{13} = -\int_0^l m_f \Psi_i \psi_j' dx \tag{13g}$$

$$M_{ij}^{22} = \int_0^l (m_0 \psi_i \psi_j + m_2 \psi_i' \psi_j') dx; \quad M_{ij}^{23} = \int_0^l (m_0 \psi_i \psi_j + m_{fz} \psi_i' \psi_j') dx; \tag{13h}$$

$$M_{ij}^{24} = \int_0^l m_g \psi_i \Psi_j dx; \quad M_{ij}^{33} = \int_0^l (m_0 \psi_i \psi_j + m_{f2} \psi_i' \psi_j') dx; \quad M_{ij}^{34} = \int_0^l m_g \psi_i \Psi_j dx \tag{13i}$$

$$M_{ij}^{44} = \int_0^l m_{g^2} \Psi_i \Psi_j dx \tag{13j}$$

and $\{\Delta\} = \{u \; w_b \; w_s \; \phi_z\}^{\mathrm{T}}$ is the eigenvector of nodal displacements corresponding to an eigenvalue.

4. Numerical Examples

Several numerical examples are carried out in this section to verify the accuracy of present theory. The effects of normal strain, lay-ups, Poisson's ratio and span-to-height ratios (L/h) on the natural frequencies and load-frequency curves of composite beams are investigated. Various boundary conditions including clamped-free (C-F), simply-supported (S-S) and clamped-clamped (C-C) beams are considered. Material properties of these examples are given in Table 1. For convenience, the following non-dimensional parameters are used:

$$\overline{P}_{cr} = \begin{cases} \dfrac{P_{cr}L^2}{E_2 bh^3} & \text{for Material 2, 3 and 6} \\[4mm] \dfrac{P_{cr}L^2}{E_1 bh^3} & \text{for Material 5} \end{cases} \tag{14a}$$

$$\overline{\omega} = \begin{cases} \dfrac{\omega L^2}{h} \sqrt{\dfrac{\rho}{E_2}} & \text{for Material 2, 3 and 6} \\[4mm] \dfrac{\omega L^2}{h} \sqrt{\dfrac{\rho}{E_1}} & \text{for Material 5} \end{cases} \tag{14b}$$

and the relative error (%):

$$\text{Error (\%)} = \frac{R_{\text{with}} - R_{\text{without}}}{R_{\text{with}}} \times 100\% \tag{15}$$

where R_{with} and R_{without} are the natural frequency obtained with and without the Poisson effect.

Example 1: Symmetric cross-ply $[90°/0°/0°/90°]$ beams (Material 1, $L/h = 2.272$ and 22.72) are considered. The first four natural frequencies and buckling loads are tabulated in Tables 2-6 along with numerical results of various higher-order beam theories (Exponential Shear Deformation Beam Theory (ESDBT) [14], Hyperbolic Shear Deformation Beam Theory (HSDBT) [18]) and quasi-3D theory [24]

(refined sinus model denoted SinRef-7p) as well as two commercial finite element softwares (ABAQUS [13] and ANSYS [24]). The differences between the results calculated by the present model and previous studies are very small. Obviously, as the axial load increases, the frequencies decrease. This happens more quickly when axial load reaches the critical buckling load (Fig. 2). The buckling occurs around P = 2.92×10^9N, 6.48×10^9N and 8.45×10^9N for C-F, S-S and C-C beams, which correspond to zero natural frequency.

Example 2: Symmetric cross-ply $[0°/90°/0°]$ and unsymmetric cross-ply $[0°/90°]$ beams (Material 2 and 3, $L/h = 5$ and 20) for various boundary conditions are analysed. The fundamental natural frequencies and critical buckling loads based on high-order beam theory (HBT) from previous research [35] are also given. The results are compared with Parabolic Shear Deformation Beam Theory (PS-DBT) ([15, 17]) and quasi-3D theories [24, 36] in Table 7. A good agreement between the present results and those of previous studies can be seen. Due to normal strain effect, for $[0°/90°/0°]$ lay-up, the present model generally gives slightly lower results than PSDBT. The effect of axial load on the natural frequencies is noticeable (Table 8). The frequencies decrease when the axial load changes from tension to compression.

Example 3: Angle-ply $[\theta/-\theta]$ and unsymmetric $[0°/\theta]$ beams for various L/h ratios are chosen (Materials 4 and 5). The natural frequencies of these beams are compared with those based on a quasi-3D theory [30] and elasticity equations using the state-space-based differential quadrature (SSDQM) [28] in Tables 9 and 10. It should be noted that both studies [28, 30] considered Poisson effect. Again, it can be seen that the present results agree well with previous studies especially with quasi-3D theory [30] and ANSYS. The natural frequencies and buckling loads decrease with the increase of fibre angle. Comparing the present results with and without the Poisson effect, there is negligible difference when $\theta = 0°$ and $90°$. However, as fibre angle changes, a significant difference is observed and the former results are smaller than latter ones. The relative errors, which are defined in Eq. (15), for two lay-ups, are plotted in Fig. 3. For $L/h = 15$, Poisson effect is stronger for angle-ply than unsymmetric lay-up, which confirm the importance of this effect for analysing composite beams. The maximum relative error is about 93.80% corresponding to $\theta = 35°$. As expected, all natural frequencies decrease when the axial load changes from tension to compression, except some third modes of angle-ply lay-up corresponding to axial mode (Tables 11 and 12). The first three mode shapes of angle-ply and unsymmetric beams with $\theta = 45°$ are presented in Fig. 4. It can be seen that the normal strain effect is more pronounced for unsymmetric than angle-ply lay-up. All three modes of unsymmetric lay-up are fourfold coupled mode (axial, bending, shear and stretching components).

Example 4: The validity and accuracy of the present theory is further investigated for sandwich

7

beams with soft core made of three layers [0°/Core/0°]. The thickness of each face is $0.1h$ and of core is $0.8h$. The results are compared with those using higher order zigzag theory (HZZT) [37, 38] in Table 13. It is observed that the solutions of the two approaches are in excellent agreement with small discrepancy even for L/h=5. The crtical buckling loads are also given in Table 14. They have not been reported before and could be served as benchmark examples for future references.

5. Conclusions

A two-noded C^1 beam element is developed for free vibration of axially loaded composite beams using a quasi-3D theory. Composite beams with various configurations including boundary conditions, span-to-height ratio and lay-ups are considered. Effects of shear, normal deformation and Poisson's ratio as well as anisotropy coupling should be simultaneously considered for the analysis of composite beams. Poisson effect is more pronounced for angle-ply than unsymmetric lay-up. The proposed beam model is found to be simply and efficient for vibration and buckling analysis of composite beams.

6. Acknowledgements

7. References

[1] T. Kant, B. S. Manjunath, Refined theories for composite and sandwich beams with C0 finite elements, Computers and Structures 33 (3) (1989) 755 – 764. doi:10.1016/0045-7949(89)90249-6.

[2] M. V. V. S. Murthy, D. R. Mahapatra, K. Badarinarayana, S. Gopalakrishnan, A refined higher order finite element for asymmetric composite beams, Composite Structures 67 (1) (2005) 27 – 35. doi:DOI: 10.1016/j.compstruct.2004.01.005.

[3] P. Vidal, O. Polit, A family of sinus finite elements for the analysis of rectangular laminated beams, Composite Structures 84 (1) (2008) 56 – 72. doi:10.1016/j.compstruct.2007.06.009.

[4] R. M. Aguiar, F. Moleiro, C. M. M. Soares, Assessment of mixed and displacement-based models for static analysis of composite beams of different cross-sections, Composite Structures 94 (2) (2012) 601 – 616. doi:10.1016/j.compstruct.2011.08.028.

[5] T. P. Vo, H.-T. Thai, Free vibration of axially loaded rectangular composite beams using refined shear deformation theory, Composite Structures 94 (11) (2012) 3379–3387. doi:10.1016/j.compstruct.2012.05.012.

[6] V. Kahya, Buckling analysis of laminated composite and sandwich beams by the finite element method, Composites Part B: Engineering 91 (2016) 126 – 134. doi:http://dx.doi.org/10.1016/j.compositesb.2016.01.031.

[7] A. S. Sayyad, Y. M. Ghugal, Bending, buckling and free vibration of laminated composite and sandwich beams: A critical review of literature, Composite Structures 171 (2017) 486 – 504. doi:http://doi.org/10.1016/j.compstruct.2017.03.053.

[8] J. R. Banerjee, Free vibration of axially loaded composite Timoshenko beams using the dynamic stiffness matrix method, Computers and Structures 69 (2) (1998) 197 – 208. doi:DOI: 10.1016/S0045-7949(98)00114-X.

[9] J. R. Banerjee, H. Su, C. Jayatunga, A dynamic stiffness element for free vibration analysis of composite beams and its application to aircraft wings, Computers and Structures 86 (6) (2008) 573 – 579, civil-Comp Special Issue. doi:DOI: 10.1016/j.compstruc.2007.04.027.

[10] A. A. Khdeir, J. N. Reddy, Free vibration of cross-ply laminated beams with arbitrary boundary conditions, International Journal of Engineering Science 32 (12) (1994) 1971–1980. doi:http://dx.doi.org/10.1016/0020-7225(94)90093-0.

[11] A. A. Khdeir, J. N. Reddy, Buckling of cross-ply laminated beams with arbitrary boundary conditions, Composite Structures 37 (1) (1997) 1–3. doi:http://dx.doi.org/10.1016/S0263-8223(97)00048-2.

[12] T. Kant, S. R. Marur, G. S. Rao, Analytical solution to the dynamic analysis of laminated beams using higher order refined theory, Composite Structures 40 (1) (1997) 1 – 9. doi:10.1016/S0263-8223(97)00133-5.

[13] M. Karama, B. A. Harb, S. Mistou, S. Caperaa, Bending, buckling and free vibration of laminated composite with a transverse shear stress continuity model, Composites Part B: Engineering 29 (3) (1998) 223 – 234. doi:DOI: 10.1016/S1359-8368(97)00024-3.

[14] M. Karama, K. S. Afaq, S. Mistou, Mechanical behaviour of laminated composite beam by the new multi-layered laminated composite structures model with transverse shear stress continuity,

International Journal of Solids and Structures 40 (6) (2003) 1525 – 1546. doi:10.1016/S0020-7683(02)00647-9.

[15] M. Aydogdu, Vibration analysis of cross-ply laminated beams with general boundary conditions by Ritz method, International Journal of Mechanical Sciences 47 (11) (2005) 1740 – 1755. doi:10.1016/j.ijmecsci.2005.06.010.

[16] M. Aydogdu, Free vibration analysis of angle-ply laminated beams with general boundary conditions, Journal of Reinforced Plastics and Composites 25 (15) (2006) 1571–1583. doi:10.1177/0731684406066752.

[17] M. Aydogdu, Buckling analysis of cross-ply laminated beams with general boundary conditions by Ritz method, Composites Science and Technology 66 (10) (2006) 1248 – 1255. doi:10.1016/j.compscitech.2005.10.029.

[18] J. Li, C. Shi, X. Kong, X. Li, W. Wu, Free vibration of axially loaded composite beams with general boundary conditions using hyperbolic shear deformation theory, Composite Structures 97 (0) (2013) 1 – 14. doi:http://dx.doi.org/10.1016/j.compstruct.2012.10.014.

[19] D. Shao, S. Hu, Q. Wang, F. Pang, Free vibration of refined higher-order shear deformation composite laminated beams with general boundary conditions, Composites Part B: Engineering 108 (2017) 75 – 90. doi:http://dx.doi.org/10.1016/j.compositesb.2016.09.093.

[20] E. Carrera, M. Filippi, E. Zappino, Free vibration analysis of laminated beam by polynomial, trigonometric, exponential and zig-zag theories, Journal of Composite Materials 48 (19) (2014) 2299–2316. arXiv:http://jcm.sagepub.com/content/48/19/2299.full.pdf+html, doi:10.1177/0021998313497775.

[21] A. Pagani, E. Carrera, M. Boscolo, J. R. Banerjee, Refined dynamic stiffness elements applied to free vibration analysis of generally laminated composite beams with arbitrary boundary conditions, Composite Structures 110 (0) (2014) 305 – 316. doi:http://dx.doi.org/10.1016/j.compstruct.2013.12.010.

[22] E. Carrera, A. Pagani, J. R. Banerjee, Linearized buckling analysis of isotropic and composite beam-columns by Carrera Unified Formulation and dynamic stiffness method, Mechanics of Advanced Materials and Structures 23 (9) (2016) 1092–1103. arXiv:http://dx.doi.org/10.1080/15376494.2015.1121524, doi:10.1080/15376494.2015.1121524.

[23] H. Matsunaga, Vibration and buckling of multilayered composite beams according to higher order deformation theories, Journal of Sound and Vibration 246 (1) (2001) 47 – 62. doi:10.1006/jsvi.2000.3627.

[24] P. Vidal, O. Polit, Vibration of multilayered beams using sinus finite elements with transverse normal stress, Composite Structures 92 (6) (2010) 1524 – 1534. doi:10.1016/j.compstruct.2009.10.009.

[25] J. L. Mantari, F. G. Canales, Free vibration and buckling of laminated beams via hybrid ritz solution for various penalized boundary conditions, Composite Structures 152 (2016) 306 – 315. doi:http://dx.doi.org/10.1016/j.compstruct.2016.05.037.

[26] F. G. Canales, J. L. Mantari, Buckling and free vibration of laminated beams with arbitrary boundary conditions using a refined HSDT, Composites Part B: Engineering 100 (2016) 136 – 145. doi:http://dx.doi.org/10.1016/j.compositesb.2016.06.024.

[27] A. Bhimaraddi, K. Chandrashekhara, Some observations on the modeling of laminated composite beams with general lay-ups, Composite Structures 19 (4) (1991) 371 – 380. doi:http://dx.doi.org/10.1016/0263-8223(91)90082-A.

[28] W. Q. Chen, C. F. Lv, Z. G. Bian, Free vibration analysis of generally laminated beams via state-space-based differential quadrature, Composite Structures 63 (3-4) (2004) 417 – 425. doi:10.1016/S0263-8223(03)00190-9.

[29] S. R. Marur, T. Kant, On the angle ply higher order beam vibrations, Computational Mechanics 40 (2007) 25–33, 10.1007/s00466-006-0079-0.

[30] J. Li, Q. Huo, X. Li, X. Kong, W. Wu, Vibration analyses of laminated composite beams using refined higher-order shear deformation theory, International Journal of Mechanics and Materials in Design (2013) 1–10doi:10.1007/s10999-013-9229-7.

[31] T. P. Vo, J. R. Banerjee, Free vibration of axially loaded composite beams using a quasi-3d theory, Proceedings of the Fifteenth International Conference on Civil, Structural and Environmental Engineering Computing (2015) 108doi:http://dx.doi.org/10.4203/ccp.108.108.

[32] T. P. Vo, H.-T. Thai, T.-K. Nguyen, F. Inam, J. Lee, Static behaviour of functionally graded sandwich beams using a quasi-3d theory, Composites Part B: Engineering 68 (0) (2015) 59 – 74. doi:http://dx.doi.org/10.1016/j.compositesb.2014.08.030.

[33] J. N. Reddy, A simple higher-order theory for laminated composite plates, Journal of Applied Mechanics 51 (4) (1984) 745–752. doi:10.1115/1.3167719.

[34] R. M. Jones, Mechanics of Composite Materials, Taylor & Francis, 1999.

[35] T. P. Vo, H.-T. Thai, Vibration and buckling of composite beams using refined shear deformation theory, International Journal of Mechanical Sciences 62 (1) (2012) 6776. doi:10.1016/j.ijmecsci.2012.06.001.

[36] J. L. Mantari, F. G. Canales, Finite element formulation of laminated beams with capability to model the thickness expansion, Composites Part B: Engineering 101 (2016) 107 – 115. doi:http://dx.doi.org/10.1016/j.compositesb.2016.06.080.

[37] A. A. Khdeir, O. J. Aldraihem, Free vibration of sandwich beams with soft core, Composite Structures 154 (2016) 179 – 189. doi:http://dx.doi.org/10.1016/j.compstruct.2016.07.045.

[38] S. Kapuria, P. C. Dumir, N. K. Jain, Assessment of zigzag theory for static loading, buckling, free and forced response of composite and sandwich beams, Composite Structures 64 (3-4) (2004) 317 – 327. doi:10.1016/j.compstruct.2003.08.013.

CAPTIONS OF TABLES

Table 1: Material properties of composite and sandwich beams.

Table 2: The first four natural frequencies and buckling loads of a cross-ply $[90°/0°/0°/90°]$ simply-supported beam (Material 1, L/h=2.272).

Table 3: The first four natural frequencies and buckling loads of a cross-ply $[90°/0°/0°/90°]$ simply-supported beam (Material 1, L/h=22.72).

Table 4: The first four natural frequencies and buckling loads of a cross-ply $[90°/0°/0°/90°]$ cantilever beam (Material 1, L/h=22.72).

Table 5: The first four natural frequencies and buckling loads of a cross-ply $[90°/0°/0°/90°]$ clamped-clamped beam (Material 1, L/h=22.72).

Table 6 The first four natural frequencies and buckling loads of a cross-ply $[90°/0°/0°/90°]$ clamped-simply supported beam (Material 1, L/h=22.72).

Table 7: The non-dimensional fundamental frequencies and critical buckling loads of $[0°/90°/0°]$ and $[0°/90°]$ composite beams (Material 2 and 3 with L/h=5 and 20).

Table 8: The non-dimensional natural frequencies of $[0°/90°/0°]$ and $[0°/90°]$ composite beams under axial load (Material 2, L/h=5 and 20).

Table 9: The fundamental frequencies of angle-ply $[\theta/-\theta]$ simply-supported beams with lay-up (Material 4, L/h=5 and 15).

Table 10: The non-dimensional fundamental frequencies of an angle-ply $[\theta/-\theta]$ and unsymmetric $[0/\theta]$ clamped-clamped beams (Material 5, L/h=5 and 15).

Table 11: The non-dimensional natural frequencies of an angle-ply $[\theta/-\theta]$ clamped-clamped beam (Material 5, L/h=5).

Table 12: The non-dimensional natural frequencies of an unsymmetric $[0°/\theta]$ clamped-clamped beam (Material 5, L/h=5).

Table 13: The non-dimensional natural frequencies of sandwich beams ($0.1h/0.8h/0.1h$, Material 6, L/h=5, 10 and 20).

Table 14: The critical buckling loads of sandwich beams ($0.1h/0.8h/0.1h$, Material 6, L/h=5, 10, 20 and 50).

Table 1: Material properties of composite and sandwich beams.

Materials	MAT 1 [14]	MAT 2 [17]	MAT 3 [17]	MAT 4 [27]	MAT 5 [28]	MAT 6 [38] (Core)	MAT 6 (Faces)
Examples	1	2		3		4	
E_1 (GPa)	241.5	40	40	181	144.8	0.2208×10^{-3}	131.1
E_2 (GPa)	18.98	1	1	10.3	9.65	0.2001×10^{-3}	6.9
E_3 (GPa)	18.98	1	1	10.3	9.65	2.76	6.9
G_{12} (GPa)	5.18	0.5	0.6	7.17	4.14	16.56×10^{-3}	3.588
G_{13} (GPa)	5.18	0.2	0.6	7.17	4.14	0.5451	3.088
G_{23} (GPa)	3.45	0.2	0.5	6.21	3.45	0.4554	2.3322
ν_{12}	0.24	0.25	0.25	0.28	0.3	0.99	0.32
ν_{13}	0.24	0.25	0.25	0.35	0.3	3×10^{-5}	0.32
ν_{23}	0.24	0.25	0.25	0.4	0.3	3×10^{-5}	0.49
ρ (kg/m^3))	2015	1	1	1389.23	1389.23	70	1000

Table 2: The first four natural frequencies and buckling loads of a cross-ply $[90°/0°/0°/90°]$ simply-supported beam (Material 1, L/h=2.272).

Mode	P=0				P=10^9 N (compression)			P$_{cr}$ (10^8N)
	ANSYS [24]	Quasi-3D [24]	ESDBT [14]	Present	ESDBT [14]	Present	ABAQUS [13]	Present
1	82.17	82.36	83.050	83.519	77.00	78.60	76.923	64.7933
2	195.22	196.45	195.501	196.504	184.44	195.05	185.382	83.3773
3	310.07	312.91	317.232	317.909	297.76	317.09	303.071	89.7520
4	424.311	429.43	453.926	451.682	422.44	441.11	435.220	98.4507

Table 3: The first four natural frequencies and buckling loads of a cross-ply $[90°/0°/0°/90°]$ simply-supported beam (Material 1, L/h=22.72).

Mode	P=0				P=10^7 N (compression)			P$_{cr}$ (10^7N)	
	ESDBT [14]	ANSYS [24]	Quasi-3D [24]	Present	ESDBT [14]	ABAQUS [13]	Present	ABAQUS [13]	Present
1	14.958	14.93	14.96	14.96	10.67	10.68	10.68	2.0381	2.0373
2	57.796	57.67	57.69	57.84	53.87	53.77	53.93	7.6407	7.6567
3	123.396	122.90	122.90	123.59	119.35	118.86	119.58	15.6844	15.6503
4	205.647	204.50	204.59	206.15	201.38	200.19	201.93	25.0822	24.6575

Table 4: The first four natural frequencies and buckling loads of a cross-ply $[90°/0°/0°/90°]$ cantilever beam (Material 1, L/h=22.72).

Mode	P=$4×10^6$N (tension)		P=0		P=$4×10^6$N (compression)		P$_{cr}$ (10^7N)
	HSDBT [18]	Present	HSDBT [18]	Present	HSDBT [18]	Present	Present
1	6.95	6.95	5.36	5.37	2.65	2.64	0.5178
2	34.64	34.64	32.57	32.57	30.34	30.34	5.4380
3	88.79	88.79	86.95	86.98	85.06	85.09	13.6591
4	162.00	162.00	160.16	160.31	158.30	158.46	19.3079

Table 5: The first four natural frequencies and buckling loads of a cross-ply [90°/0°/0°/90°] clamped-clamped beam (Material 1, L/h=22.72).

Mode	P=2×10⁷N (tension)		P=0		P=2×10⁷N (compression)		P_{cr} (10⁷N)
	HSDBT [18]	Present	HSDBT [15]	Present	HSDBT [18]	Present	Present
1	36.36	36.37	32.54	32.56	28.13	28.15	7.6617
2	90.14	91.38	84.57	85.84	78.56	79.89	14.4530
3	161.57	161.81	155.02	155.30	148.17	148.50	24.6648
4	245.79	248.32	238.39	241.02	230.74	233.48	32.8958

Table 6: The first four natural frequencies and buckling loads of a cross-ply [90°/0°/0°/90°] clamped-simply supported beam (Material 1, L/h=22.72).

Mode	P=2×10⁷N (tension)		P=0		P=2×10⁷N (compression)		P_{cr} (10⁷N)
	HSDBT [18]	Present	HSDBT [15]	Present	HSDBT [18]	Present	Present
1	16.47	16.57	22.95	23.04	27.87	27.97	4.0779
2	64.07	64.38	70.97	71.24	77.23	77.49	11.1194
3	131.90	132.48	139.36	139.88	146.43	146.90	19.8446
4	214.34	215.25	222.43	223.25	230.22	230.97	28.9888

Table 7: The non-dimensional fundamental frequencies and critical buckling loads of $[0°/90°/0°]$ and $[0°/90°]$ composite beams (Material 2 and 3 with L/h=5 and 20).

Lay-ups	Reference	Material 2				Material 3			
		Frequencies		Buckling loads		Frequencies		Buckling loads	
		L/h=5	20	5	20	5	20	5	20
C-F beams									
$[0°/90°/0°]$	PSDBT [15, 17]	4.233	6.070	4.708	7.611	-	-	3.717	7.408
	Quasi-3D (SinRef-7p) [24]	4.189	-	-	-	-	-	-	-
	Quasi-3D [36]	4.222	-	4.378	-	-	-	-	-
	Present (HBT)	4.230	6.062	4.704	7.600	3.660	5.921	3.714	7.397
	Present (Quasi-3D)	4.221	6.063	4.362	7.593	3.653	5.922	3.491	7.391
$[0°/90°]$	PSDBT	2.384	2.590	1.236	1.349	-	-	1.175	1.344
	Quasi-3D (SinRef-7p) [24]	2.289	-	-	-	-	-	-	-
	Quasi-3D [36]	2.375	-	1.213	-	-	-	-	-
	Present (HBT)	2.381	2.589	1.234	1.347	2.292	2.580	1.174	1.342
	Present (Quasi-3D)	2.391	2.598	1.226	1.356	2.301	2.590	1.166	1.351
S-S beams									
$[0°/90°/0°]$	PSDBT [15, 17]	9.207	16.337	8.613	27.084	-	-	5.896	24.685
	Quasi-3D (SinRef-7p) [24]	9.201	-	-	-	-	-	-	-
	Quasi-3D [36]	9.208	-	8.556	-	-	-	-	-
	Present (HBT)	9.206	16.327	8.609	27.050	7.622	15.590	6.278	24.830
	Present (Quasi-3D)	9.208	16.328	8.524	27.073	7.624	15.591	5.856	24.674
$[0°/90°]$	PSDBT [15, 17]	6.144	7.218	3.906	5.296	-	-	3.376	5.225
	Quasi-3D (SinRef-7p) [24]	5.671	-	-	-	-	-	-	-
	Quasi-3D [36]	6.109	-	3.939	-	-	-	-	-
	Present (HBT)	6.058	7.204	3.903	5.330	5.672	7.156	3.373	5.219
	Present (Quasi-3D)	6.075	7.228	3.946	5.330	5.684	7.179	3.404	5.257
C-C beams									
$[0°/90°/0°]$	PSDBT [15, 17]	11.637	29.926	-	-	-	-	-	-
	Quasi-3D (SinRef-7p) [24]	11.100	-	-	-	-	-	-	-
	Quasi-3D [36]	11.499	-	11.306	-	-	-	-	-
	Present (HBT)	11.601	29.643	11.648	75.257	9.547	26.106	7.809	59.472
	Present (Quasi-3D)	11.479	29.639	11.053	75.312	9.474	26.102	7.509	59.463
$[0°/90°]$	PSDBT [15, 17]	10.103	15.688	-	-	-	-	-	-
	Quasi-3D (SinRef-7p) [24]	8.743	-	-	-	-	-	-	-
	Quasi-3D [36]	9.985	-	8.660	-	-	-	-	-
	Present (HBT)	10.022	15.650	8.670	19.757	8.741	15.205	6.574	18.801
	Present (Quasi-3D)	9.990	15.708	8.502	19.951	8.710	15.258	6.474	18.974

Table 8: The non-dimensional natural frequencies of $[0°/90°/0°]$ and $[0°/90°]$ composite beams under axial load (Material 2, L/h=5 and 20).

Lay-ups	L/h	P=-0.5P$_{cr}$(tension)			P=0			P=0.5P$_{cr}$ (compression)		
		ω_1	ω_2	ω_3	ω_1	ω_2	ω_3	ω_1	ω_2	ω_3
C-F beams										
$[0°/90°/0°]$	5	4.931	16.083	30.629	4.221	14.359	28.224	3.240	12.270	25.375
	20	7.257	33.337	75.420	6.063	31.724	73.740	4.405	30.005	72.018
$[0°/90°]$	5	2.844	11.444	24.418	2.391	10.774	23.685	1.753	10.043	22.903
	20	3.125	16.356	42.307	2.598	15.701	41.728	1.875	15.013	41.141
S-S beams										
$[0°/90°/0°]$	5	11.246	24.971	39.646	9.208	21.423	34.945	6.530	16.935	28.876
	20	19.997	59.122	105.821	16.328	54.440	100.011	11.546	49.312	93.834
$[0°/90°]$	5	7.425	19.634	24.544	6.075	17.919	24.301	4.304	15.860	24.098
	20	8.852	29.522	60.534	7.228	27.730	58.651	5.111	25.813	56.703
C-C beams										
$[0°/90°/0°]$	5	13.833	28.602	44.185	11.479	24.318	38.733	8.336	18.553	31.163
	20	35.827	79.478	124.236	29.639	68.933	109.591	21.399	56.225	92.553
$[0°/90°]$	5	12.047	25.786	39.530	9.990	22.191	34.873	7.245	17.546	28.647
	20	19.056	46.223	80.253	15.708	41.254	74.331	11.242	35.512	67.868

Table 9: The fundamental frequencies of angle-ply $[\theta/-\theta]$ simply-supported beams (Material 4, L/h=5 and 10).

L/h	Reference	$0°$	$15°$	$30°$	$45°$	$60°$	$75°$	$90°$
5	Present*	5773.71	5572.33	4951.80	3916.79	2723.52	1996.69	1863.43
	Present	5764.75	4329.13	2980.61	2336.17	2032.39	1897.56	1859.47
10	Quasi-3D* [30]	1823.30	1731.70	1470.00	1092.10	721.20	517.60	481.60
	Quasi-3D [30]	1819.70	1226.60	793.70	610.00	526.90	490.70	480.50
	ANSYS [30]	1823.20	1241.00	803.20	614.94	529.60	492.51	482.17
	Present*	1822.52	1730.75	1468.96	1091.43	720.91	517.34	481.36
	Present	1818.97	1226.39	793.61	609.90	526.75	490.46	480.30

*Poisson effect is neglected

Table 10: The non-dimensional fundamental of angle-ply $[\theta/-\theta]$ and unsymmetric $[0/\theta]$ clamped-clamped beams (Material 5, L/h=5 and 15).

L/h	Lay-ups	Reference	$0°$	$15°$	$30°$	$45°$	$60°$	$75°$	$90°$
5	$[\theta/-\theta]$	Present*	2.4505	2.4025	2.2602	2.0133	1.6544	1.3893	1.3510
		Present	2.4448	2.0785	1.6668	1.4409	1.3546	1.3428	1.3477
	$[0°/\theta]$	Present*	2.4505	2.4266	2.3588	2.2501	2.1075	2.0125	1.9983
		Present	2.4448	2.2820	2.1200	2.0343	1.9999	1.9928	1.9935
15	$[\theta/-\theta]$	SSDQM [28]	4.8575	3.6113	2.3016	1.8145	1.6686	1.6200	1.6237
		Present*	4.9122	4.7165	4.1294	3.1993	2.2076	1.6895	1.6276
		Present	4.9004	3.2912	2.1832	1.7621	1.6249	1.6117	1.6227
	$[0°/\theta]$	SSDQM [28]	4.8575	4.1899	3.3548	2.9814	2.9491	2.8002	2.8012
		Present*	4.9122	4.8131	4.4994	3.9415	3.2748	2.9221	2.8805
		Present	4.9004	3.9967	3.2489	2.9575	2.8669	2.8615	2.8709

*Poisson effect is neglected

Table 11: The non-dimensional natural frequencies of an angle-ply $[\theta/-\theta]$ clamped-clamped composite beam under axial load (Material 5, L/h=5).

fibre angle	P_{cr}	P = -0.5P$_{cr}$ (tension)			P = 0 (no axial force)			P = 0.5P$_{cr}$(compression)		
		ω_1	ω_2	ω_3	ω_1	ω_2	ω_3	ω_1	ω_2	ω_3
0°	0.5148	2.9517	6.1096	9.3689	2.4448	5.1681	8.0872	1.7720	3.9234	6.3491
15°	0.3770	2.5092	5.3110	8.0786	2.0786	4.5305	6.9899	1.5078	3.5284	5.5511
30°	0.2413	2.0123	4.4232	5.6171	1.6669	3.8400	5.6171	1.2062	3.1205	5.6171
45°	0.1803	1.7413	3.8974	4.4963	1.4412	3.4139	4.4963	1.0401	2.8281	4.4963
60°	0.1601	1.6383	3.6825	4.1762	1.3551	3.2355	4.1762	0.9767	2.6972	4.1762
75°	0.1585	1.6251	3.6448	4.1950	1.3438	3.2038	4.1950	0.9682	2.6724	4.1950
90°	0.1603	1.6317	3.6513	4.2520	1.3492	3.2096	4.2520	0.9720	2.6763	4.2520

Table 12: The non-dimensional natural frequencies of an unsymmetric $[0°/\theta]$ clamped-clamped beam under axial load (Material 5, L/h=5).

fibre angle	P_{cr}	P = -0.5P$_{cr}$ (tension)			P = 0 (no axial force)			P = 0.5P$_{cr}$(compression)		
		ω_1	ω_2	ω_3	ω_1	ω_2	ω_3	ω_1	ω_2	ω_3
0°	0.5148	2.9517	6.1096	9.3689	2.4448	5.1681	8.0872	1.7720	3.9234	6.3491
15°	0.4512	2.7554	5.7638	8.7871	2.2822	4.8958	7.6020	1.6546	3.7622	5.9937
30°	0.3887	2.5595	5.4529	8.3033	2.1202	4.6724	7.2702	1.5361	3.6713	5.8814
45°	0.3580	2.4564	5.2794	8.0171	2.0346	4.5449	7.0851	1.4729	3.6098	5.8146
60°	0.3469	2.4155	5.2006	7.8440	2.0003	4.4845	6.9848	1.4473	3.5732	5.7625
75°	0.3456	2.4075	5.1755	7.7068	1.9933	4.4647	6.9329	1.4419	3.5565	5.7279
90°	0.3464	2.4087	5.1696	7.5383	1.9942	4.4614	6.9004	1.4424	3.5521	5.7104

Table 13: The non-dimensional natural frequencies of sandwich beams ($0.1h/0.8h/0.1h$, Material 6, L/h=5, 10 and 20).

L/h	Mode	Simply-Supported			Clamped-Clamped		Clamped-Free	
		HZZT [38]	HZZT [37]	Present	HZZT [37]	Present	HZZT [37]	Present
5	1	7.823	7.842	8.014	9.257	9.302	3.675	3.722
	2	17.274	17.402	17.695	18.890	19.029	11.906	11.982
	3	26.903	27.362	27.441	29.607	29.061	22.542	22.543
	4	36.937	38.152	37.599	41.178	39.824	32.824	30.343
10	1	12.237	12.249	12.428	16.534	16.814	5.073	5.114
	2	31.291	31.366	32.057	33.641	35.285	19.529	19.813
	3	50.218	50.441	51.511	52.924	53.521	39.878	40.516
	4	69.096	69.607	70.781	72.532	73.256	59.219	60.054
20	1	15.382	15.387	15.477	26.377	26.764	5.790	5.806
	2	48.948	48.995	49.711	57.193	60.800	28.745	29.080
	3	86.902	87.044	88.774	92.952	94.706	64.737	65.774
	4	125.160	125.464	128.228	130.272	133.777	102.922	104.867

Table 14: The critical buckling loads of sandwich beams ($0.1h/0.8h/0.1h$, Material 6, L/h=5, 10, 20 and 50).

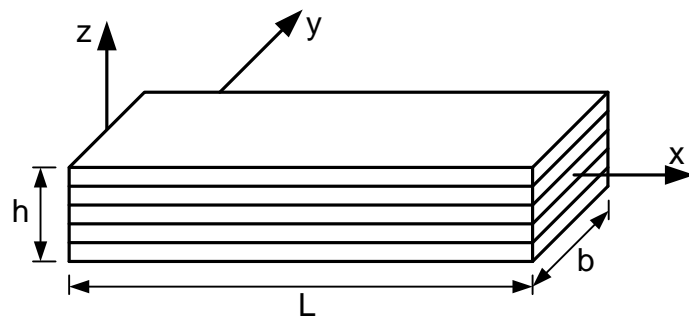| Boundary conditions	5	10	20	50
Simply-Supported	1.669	4.028	6.233	7.363
Clamped-Clamped	2.008	6,676	16.111	26.691
Clamped-Free	0.950	1.548	1.805	1.890

CAPTIONS OF FIGURES
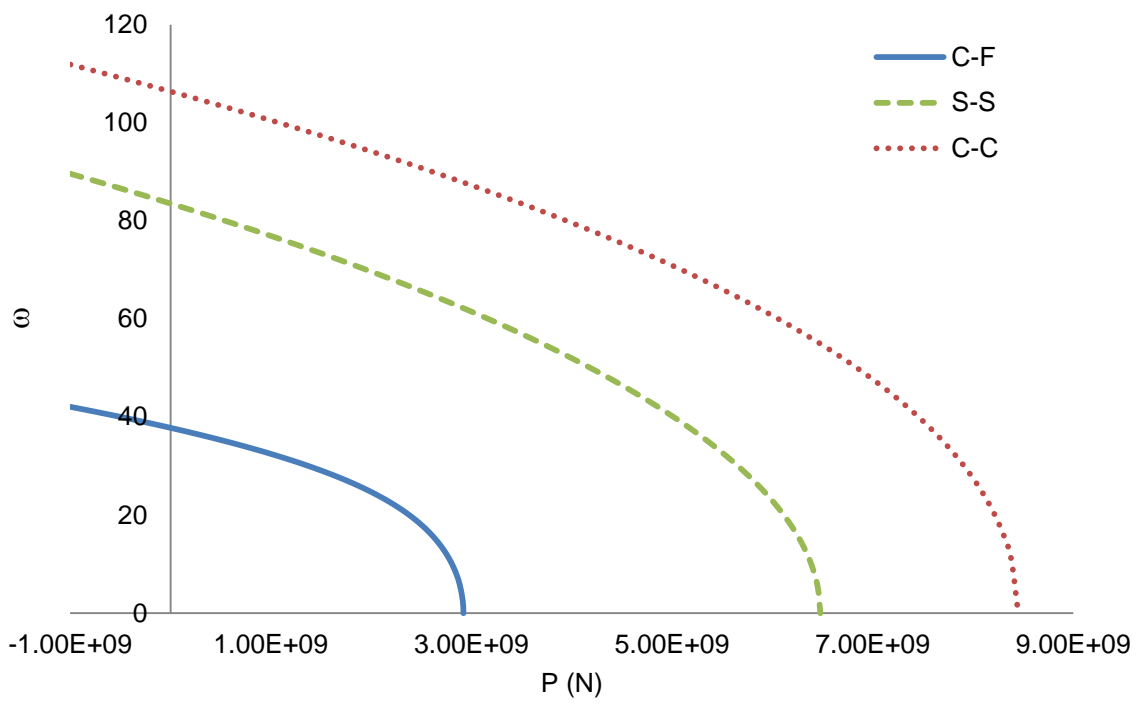
Figure 1: Geometry of a laminated composite beam.

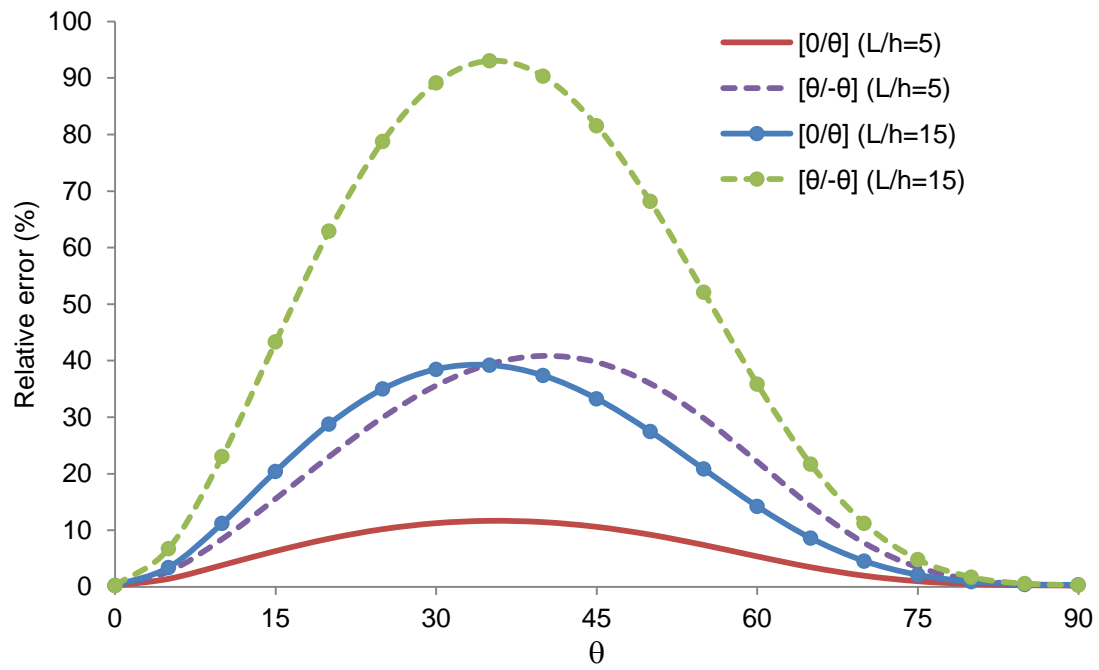Figure 2: Load-frequency curves of $[90^0/0^0/0^0/90^0]$ beams with various boundary conditions (Material 1, L/h=2.272).
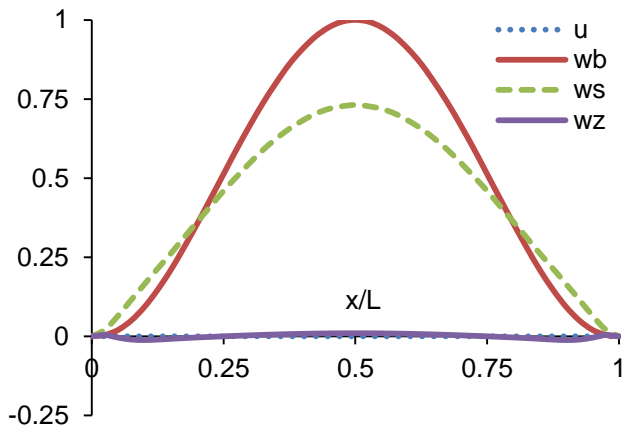
Figure 3: Relative error (%) between the results with and without the Poisson effect of clamped-clamped composite beams with $[\theta/-\theta]$ and $[0/\theta]$ lay-up (Material 5, L/h=5 and 15).
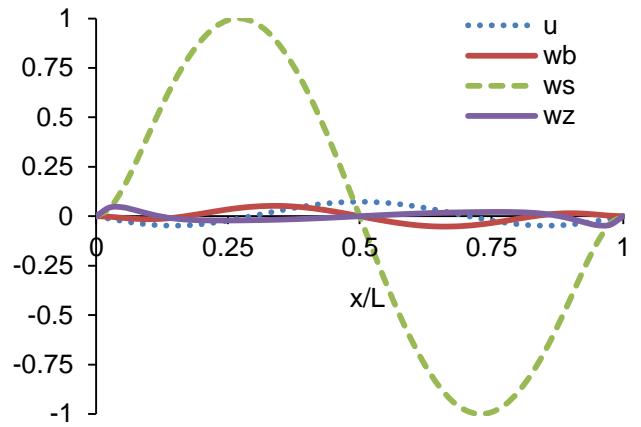
Figure 4: Vibration mode shapes of angle-ply and unsymmetric clamped-clamped composite beams under compression ($P = 0.5P_{cr}$) with the fiber angle 45^0

Figure 1: Geometry of a laminated composite beam.

Figure 2: Load-frequency curves of $[90^0/0^0/0^0/90^0]$ beams with various boundary conditions (Material 1, L/h=2.272).

Figure 3: Relative error (%) between the results with and without the Poisson effect of clamped-clamped composite beams with [θ/-θ] and [0/θ] lay-up (Material 5, L/h=5 and 15).

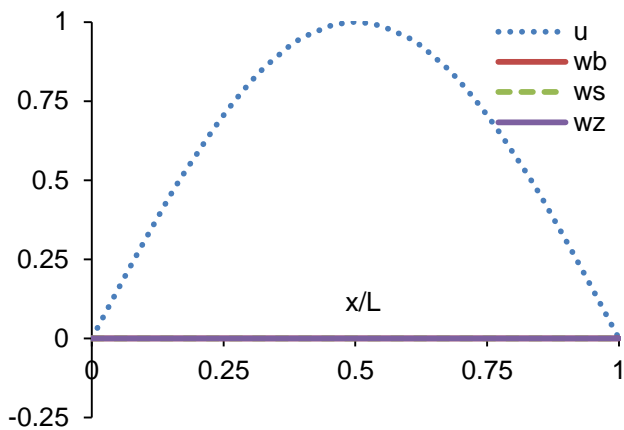a. First mode shape $\omega_1 = 1.0401$ ([θ/-θ] lay-up)
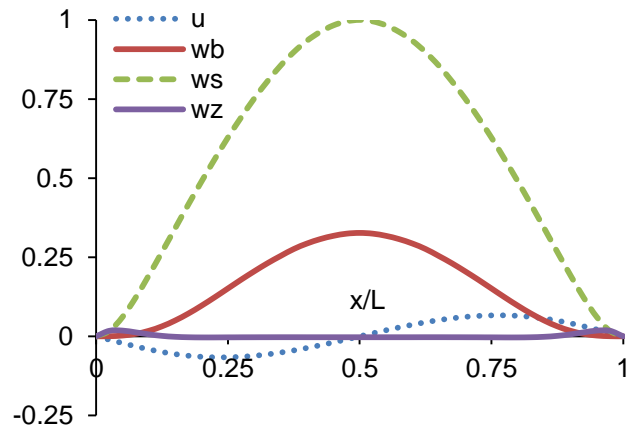
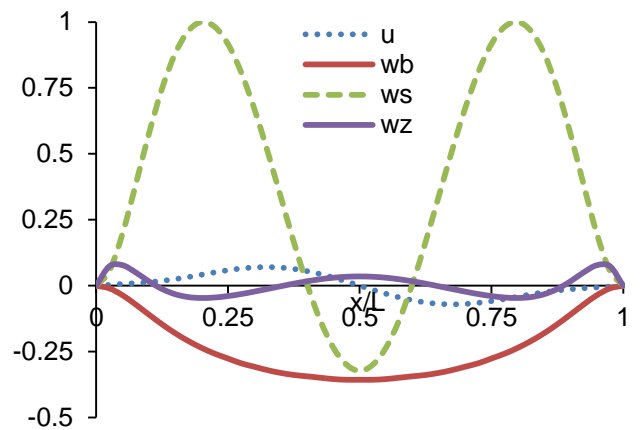a. First mode shape $\omega_1 = 1.4729$ ([0/θ] lay-up)
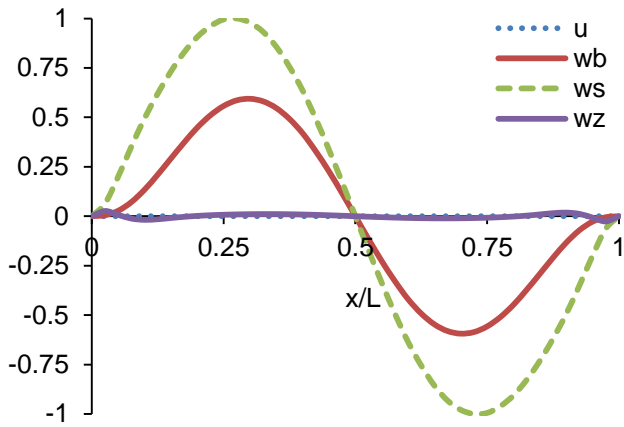
b. Second mode shape $\omega_2 = 2.8281$ ([θ/-θ] lay-up)

b. Second mode shape $\omega_2 = 3.6098$ ([0/θ] lay-up)

c. Third mode shape $\omega_3 = 4.4963$ ([θ/-θ] lay-up)

c. Third mode shape $\omega_3 = 5.8146$ ([0/θ] lay-up)

Figure 4: Vibration mode shapes of angle-ply and unsymmetric clamped-clamped composite beams

under compression (P = 0.5P$_{cr}$) with the fiber angle 45^0